

Methodology for EDF's Permian Methane Analysis Project (PermianMAP)

Data Collection and Analysis

Last Updated: November 17, 2021

[Aerial Surveys: University of Arizona / NASA Jet Propulsion Laboratory / CarbonMapper](#)

Data Collection

University of Arizona (U. Arizona) and NASA Jet Propulsion Laboratory (NASA-JPL) performed an extensive aerial survey of methane point sources over the Permian basin in September-November 2019. Complete details about the methodology in the form of peer-reviewed publications are available for this campaign in the Permian¹, prior campaigns in other regions^{2,3} and a controlled release study⁴. In brief, the Airborne Visible-Infrared Imaging Spectrometer - Next Generation (AVIRIS-NG) instrument is installed on an aircraft and flown in a lawnmower pattern to systematically image point source emissions of CH₄. This platform enables repeated, high-resolution mapping of vast areas for large CH₄ emission sources. In total, the Fall 2019 Permian campaign detected 3067 plumes of methane above the 10-20 kg/hr detection limit. Plumes detected on repeated overflights were aggregated within an 150m spatial buffer to 1756 unique 'sources' in order to attribute the plumes to specific facilities and assess their persistence.

The persistence of each source is calculated as the number of unique days in which a plume was detected at a source divided by the number of days in which the aircraft surveyed that location. In many instances, the aircraft captured multiple plumes from the same source separated by less than an hour – these are not considered repeat detections for the purpose of persistence calculations. Reported 'persistence weighted emissions' of each source are expressed as the average of all plumes detected from a location multiplied by the fractional persistence value. All sources were manually inspected using a combination of high-resolution imagery collected by the aircraft and Google Earth satellite imagery to determine the segment of O&G production responsible: Production (well, tank), Gathering & Boosting (compressor, pipeline) and Processing. Data from this campaign as collected by U. Arizona and NASA-JPL are directly available via the Methane Source Finder⁵. Questions related to the instrument methodology and data collection can be sent to msf@jpl.nasa.gov.

Beginning in July 2021, the AVIRIS-NG instrument was installed on the Global Atmospheric Observatory (GAO) aircraft in coordination with CarbonMapper⁶. Mapping flights of predetermined regions in both

Delaware (~5000 km²) and Midland (~2500 km²) sub-basins occurred between July 25 and August 10, 2021. Flights occurred on all days with acceptable atmospheric conditions with the intent to map all predetermined regions at least three times during the flight window. Preliminary plume data was distributed to operators and published on PermianMAP in August 2021 incorporating coarse estimates of hourly averaged wind speed from the nearest TX and NM ASOS network⁷ stations to derive preliminary emission rates. Final quality control (QC) on data from the Summer 2021 flights has been conducted in September 2021 and re-submitted to operators. This final QC includes quantitative estimates of emission rates using the High-Resolution Rapid Refresh (HRRR)⁸ wind product as in the established methodology from past campaigns¹⁻³. This finalized dataset includes spatiotemporal information and emission rate estimates from 929 plumes emanating from 533 unique locations in the target regions. This finalized dataset has replaced the preliminary data on the operator dashboard and data download sections of the PermianMAP platform⁹.

The GAO aircraft was again deployed to the Permian Basin for another flight campaign on all days with acceptable meteorological conditions between October 3rd and 17th, 2021. The flight pattern for these flights (referred to as Fall 2021 campaign) followed the same general region as the Summer 2021 campaign conducted two months prior, albeit with minor adjustments to the exact number of daily overflights for each sub-region. Shapefiles of the precise regions covered by the aircraft including how many days each region was flown during both 2021 campaigns are available from the data download section of the PermianMAP platform⁹. Unlike for the Summer 2021 campaign, no preliminary emission rates were distributed or published for the Fall 2021 campaign. Finalized QC emission rates were distributed to operators on November 8, 2021 following the attribution methodology as described below. In this campaign 773 emission plumes were identified to emanate from 457 unique sources. Despite the reduction in plume and source counts in the Fall vs Summer 2021 campaigns, preliminary analyses indicate the total aggregated persistence-adjusted emissions detected from the two campaigns agree within uncertainty at ~80 metric tons per hour. Further analyses are ongoing regarding the comparison of separate aerial remote sensing campaigns.

Operator Attribution

After receiving the data from U. Arizona and NASA-JPL, EDF attributed the observed plumes and emission sources to the most likely responsible operators for each source based on the distance to known wells, midstream sites and pipeline infrastructure. Wellsite locations were provided by Enverus DrillingInfo¹⁰, using information reported by operators to Texas¹¹ and New Mexico¹² state agencies. Operator attribution only considered wellsites that were active during the months of September-November 2019. Some locations of midstream facilities were provided by Enverus Prism and DrillingInfo¹⁰, while others were interpreted by Air Permitting and Emission Inventory databases from New Mexico (NMED)¹³ and Texas (TCEQ)¹⁴ environmental agencies. Pipeline ownership was determined by Enverus DrillingInfo¹⁰. In cases where the ownership was ambiguous from limited data or adjacent sites the ownership was labeled as 'UNKNOWN'. Charts and tables on the operator dashboard aggregate emissions by operators using the persistence weighted emissions values for each source and only include those sources with at least 3 overflights by the aircraft. Questions regarding facility ownership

can be addressed using the online form in the 'Submit A Response' section of the PermianMAP platform⁹.

Operator attribution for the 2021 campaigns proceeded as described above, with the only change being utilization of the most recently available updates to the ownership of wellsites, midstream facilities and pipelines. Through the process of attributing emission events to operators in the Summer 2021 dataset, several sources from the 2019 dataset were determined to have incorrect operator attributions and have been revised in the current version available on the operator dashboard and in the data download section of the platform⁹. Any additional revisions of operator ownership based on feedback from operators or additional QC will be updated when available. As of November 17 2021, all operator ownership correction forms submitted to the online platform have been updated within the dashboard and downloadable datasets.

Aerial Surveys: Scientific Aviation

Data Collection

Scientific Aviation quantifies methane emissions at various spatial scales from a cluster of a few well pads (~3-15 km²) to the entire Delaware basin study area (10,000 km²) using the aerial mass balance approach¹⁵. In brief, a single-engine Mooney aircraft is outfitted with a Picarro CRDS instrument (G2210-m) to measure in-situ atmospheric CH₄, CO₂ and H₂O mole fractions, a differential GPS and aircraft data computer to enable computation of horizontal wind speeds and directions and a Vaisala probe to measure ambient temperature and relative humidity. These in-flight measurements are synthesized to estimate a snapshot of methane emissions from the areas circumscribed by the plane. Based on earlier controlled release experiments, the detection limit of the mass balance approach can be as low as 5–10 kg CH₄/hr; however, the exact detection limit is highly dependent on dynamic parameters such as upwind methane concentration and local meteorology (see section 'Uncertainty, Detection Limits and Scale' below for more details).

For PermianMAP, Scientific Aviation was deployed for three types of measurements: regional mass balances (described in greater detail in the section 'Aircraft Based Regional Emissions Quantification'), box mass balances and site cluster mass balances. Box mass balances occurred systematically around 25 pre-defined 20x20 km boxes within our 100 x 100 km Delaware basin study area. Site cluster mass balances were measurements of emission plume(s) from near ground level to their vertical extent, captured from 1-2 km radius spiral flights. These areas were selected using two strategies based on the observations from 20x20 km boxes: randomly selected locations and randomly selected single-operator clusters. For each 20x20 km box, five to ten 2x2 km sub-grids were randomly selected; these areas often contain wells from multiple operators. For the second approach, pre-defined irregular shapes in each 20x20 km box were assigned based on a geospatial analysis that clustered wells into single operator groups. For each 20x20 box, several of these single operator areas were randomly selected for mass balance measurements.

PermianMAP publishes Scientific Aviation data that have passed quality assurance. New data will be added from both additional flights and quality assurance of existing data. While a best effort has been made to provide accurate emission estimates, all data should be considered preliminary and subject to change.

Attributing Wells to Emission Events

Several well characteristics are used to determine wells associated with an aerial cluster emission event observation. The well must have been actively in operation or actively producing during our study period (October 2019 – present) and must have a first production date prior to the given emission event. This allows us to maintain up-to-date well data while avoiding associating new wells with older emission events. Well datasets of actively producing wells are updated on a monthly cadence based on the data reported by operators to Texas¹¹ and New Mexico¹² state agencies. Attributed wells are a potential source of a given emission event; however, it is possible that midstream facilities or pipelines are responsible. Tank battery locations displayed on PermianMAP are based on satellite imagery analysis by Descartes Labs¹⁶ and locations of Gas Processing Plants are provided by the EPA Greenhouse Gas Reporting Program¹⁷. Plans to incorporate additional midstream facilities are underway and will be released at a later date.

Ground Surveys: University of Wyoming

Data Collection

The University of Wyoming (UW) team quantifies site-level methane and VOC emissions using two vehicle-based approaches: Other Test Method 33A (OTM) and the transect method. OTM is an inverse Gaussian dispersion method developed by the US EPA¹⁸. In summary, a vehicle equipped with a pollutant sensor and 3D sonic anemometer is deployed 40–200 meters downwind of an emission source for approximately 20 minutes at a stationary location near the plume centerline. Site-level emission rates are estimated by fitting concentration and wind data to a Gaussian curve^{19, 20}. The transect method uses the same vehicle-based measurement platform, but samples the plume as the vehicle drives back and forth on a downwind road in a direction transverse to wind²¹. The precision of OTM and transect methods (for 10+ passes) has been estimated to be +233%/-41% and +170%/-50%, respectively^{21, 22}.

In January 2020, UW deployed their mobile air quality laboratory to the study area to perform OTM and transect measurements at randomly selected well pads and tank batteries. Methane and speciated VOCs were measured continuously with a Picarro CRDS and PTR-TOF-MS^{21, 22}. Site selection followed a pseudo-random process that accounted for the methodological constraint of downwind public road access. Several 20x20 km areas were randomly selected within our gridded 100x100 km area, excluding any area with limited public roads. The UW team randomly selected sites within each 20x20 km area for OTM and/or transect measurements that were downwind of the current wind direction. In addition to quantifying emissions, the UW team used a FLIR camera to inspect the site for emissions from the fence line. At some sites, a canister air sample was collected for VOC analysis to supplement PTR-TOF-MS data²³. For sites where it was confirmed that the mobile laboratory was downwind of the site, but no

enhanced methane was detected for at least 10 minutes, emissions were reported as Below Detection Limit (BDL), which has been estimated as 0.036 kg CH₄/hr for the OTM method¹⁹.

In October-November 2020, UW again deployed their mobile air quality laboratory to collect additional OTM and transect measurements from Permian Basin well pads. Owing to limited access on public lease roads in Texas, UW focused on public lands managed by the New Mexico State Trust Land Office and the Federal Bureau of Land Management. Additionally, focus was emphasized within the sampling scheme to capture more measurements on marginal (or stripper) wells in order to fill gaps in the literature on this well type. Although the exact classification depends on the agency, for this survey, the team defined marginal wells as those with an annual average production rate of less than 15 Barrels-of-oil equivalent per day.

OGI Surveys of Emissions from Flaring & Other Equipment

Site Selection and Protocol:

EDF compiled a list of potential locations of recently active flares in the Permian region (Delaware and Midland Basins) based on a geospatial analysis of the SkyTruth Global Flaring Dataset²⁴. This dataset utilizes VIIRS Nightfire (VNF) nightly data produced by the Earth Observation Group, Payne Institute for Public Policy, Colorado School of Mines²⁵⁻²⁷. To account for the spatial uncertainty of the detections from the VIIRS instrument, the individual flare detections from October 1 2019 to January 31 2020 were spatially joined using a 100-meter buffer distance and the centroid location of the 1,014 joined detections were defined as likely locations of recently active O&G flares.

Leak Surveys Incorporated (LSI)²⁸, a leak detection company specializing in aerial optical gas imaging, was provided a list of 573 potential active flare locations from the original set of 1,014. Site selection balanced representativeness and efficiency by defining one contiguous, high flare density area in each basin that could be surveyed in a total of approximately five days. For the Delaware, 323 locations were selected corresponding to part of the main 100 x 100 km² PermianMAP Delaware basin study area defined by the NW and SE corners 32.325° N, 103.822° W and 31.417° N, 103.202° W, plus three additional flares on University Lands located within 6 km of the study area. For the Midland, 250 locations were selected from the two counties with the highest flare counts: Midland and Martin.

LSI surveyed these locations with a custom infrared camera (IR) deployed in a R44 helicopter. Flare locations were identified with a latitude/longitude and unique flare ID. During the week of February 17, 2020 (Survey 1), LSI surveyed the selected 573 potential flare locations to determine the presence of a flare; if a flare was identified near the spatial coordinates, LSI recorded 15 – 30 seconds of both visual spectrum and IR video of the flare and nearby equipment. For flares with apparent combustion issues, LSI recorded an additional 30 – 60 seconds of footage of the flare plume from multiple angles to provide visual evidence of flare status. For each flare, LSI assigned a qualitative assessment of the apparent flare status at the time of survey from four categories: inactive and unlit with no emissions (inactive); active, lit and operating properly (operational); active and lit but with operational issues such as incomplete combustion or excessive smoke (combustion issues); or active, unlit and venting methane (unlit and venting). If multiple flares were present at approximately the same distance from the reported

coordinates, then LSI randomly selected a flare to assign to the Flare ID. If no active or inactive flares were visible from the reported coordinates, then the team reported no flare was present at the location.

During the week of March 23, 2020 (Survey 2), LSI was deployed for a follow-up survey at 337 flare locations: all of the malfunctioning or unlit flares from Survey 1 plus a random selection of half the operational or inactive flares from the first survey. LSI used a similar protocol as the first survey, but only recorded video for flares with a malfunctioning or unlit status. Additionally, LSI was deployed to systematically survey all O&G flares in a 20 x 20 km box defined by the NW and SE corners 31.780° N, 103.406° W and 31.596° N, 103.199° W (referred to as the Systematic Survey). A third flaring survey occurred from June 22 – July 1, 2020 with a similar methodology to the second survey for repeated observations of problematic flares and random sampling of the identified flares. The systematic survey was also repeated during Survey 3.

LSI was deployed for a fourth survey during the Week of November 2-7, 2020. During this survey, the ‘Random’ protocol was repeated; however, a new batch of sites was selected using a geospatial analysis of the VIIRS Nightfire^{24, 27} detections from July 1, 2020 to October 15, 2020. Simultaneously alongside this deployment, an ~200km² area with a high density of active flares in the counties of Loving TX and Lea, NM was targeted for a ‘Repeat Area’ Survey. Here, LSI recorded the status of all flares three times on the days of November 2nd, 4th and 6th 2020 to assess the variability in flare performance at the scale of a week.

LSI was deployed for a fifth survey during the Week of April 13-18 2021. During this survey, instead of focusing entirely on flaring malfunctions, the protocol was expanded to explore all visible emission points using their helicopter-OGI platform similar to an extensive survey across several major US O&G basins²⁹. Three different survey protocols were followed during 6 survey days. First, for ~2.5 days the helicopter systematically surveyed all wellpads within two pre-defined areas containing a high diversity of wellsite characteristics (old vs new, and high vs low production). Additionally, ~2.5 days were spent targeting sites presumed to be ‘complex marginal wellpads’ as identified using satellite imagery and production data¹⁰. In this context, complex wellpads are those containing additional infrastructure beyond a pumpjack or wellhead (e.g. tanks, separators, compressors, etc.). During the source of these two surveys, LSI dropped a GPS pin at each complex site surveyed and recorded the count of all tanks, flares, compressors, wellheads or pumpjacks for later data processing and analytics. During the 6th and final day of the survey, a protocol similar to the prior ‘Random’ flaring surveys was repeated; however, again a new batch of sites to survey was selected using a geospatial analysis of the VIIRS Nightfire^{24, 27} detections from Mar 15, 2021 to April 8, 2021 to most accurately capture the locations of routine flaring during the preceding month.

LSI was deployed to the Permian again during August 3-8 2021 (Survey 6), this time assessing the prevalence of flaring malfunctions and other emission sources at Midstream sites throughout the basin – predominantly compressor stations and processing plants. For this survey (and all future ones), a new camera³⁰ with ~4x pixel resolution and increased sensitivity was mounted onboard the R44 helicopter with a custom gimbal setup for image stabilization. Observations of emissions are available on the flaring dashboard and data download sections of the PermianMAP website.

LSI was again deployed to the Permian during September 27 – October 5 2021 for a 7th survey. Approximately 5 days of this survey were spent continuing to collect observations of emissions and unlit flares at compressor stations and processing plants, spanning much wider regions of the Permian Basin than what was covered in prior surveys. Additionally, on this deployment, 2 days were spent targeting specific complex wellpads to collect more information about the prevalence of and distribution of wellpad emission sources, while one day was spent revisiting persistent emissions sources from pipelines detected during the Summer 2021 CarbonMapper campaign.

OGI Observations and Performance Results:

For Survey 1, LSI found 337 flares at the provided locations, 312 of which were active during the survey. About 11% of flares had issues that could cause abnormally high methane emissions: 7.4% were lit but with combustion issues while 4.2% were unlit and venting. For Surveys 2 and 3, all malfunctioning flares during the prior surveys were revisited and additional flares from the list of target sites were sampled with the time remaining. Overall, the results were similar to the first survey with an ~11% malfunction rate, although a higher proportion of the malfunctioning flares were unlit and venting on the second survey as compared with the others. Nine flares were observed to be malfunctioning during the first two surveys occurring about 5 weeks apart, while two flares were found to be malfunctioning during all three surveys (Flare ID 448 and 630) which spanned about 4 months. The results from the 4th survey on a completely independent list of target sites found a similar rate of flare malfunctions (4.4%) albeit a smaller rate of combustion issues (3.1%).

Table 1: Summary of ‘Random’ Flaring Survey Observations

	Survey 1	Survey 2	Survey 3	Survey 4	Average
Operational	276	147	237	294	
Inactive	25	0	62	47	
Combustion Issue	23	9	18	10	
Unlit and Venting	13	10	12	14	
Not Surveyed	94	265	102	0	
Active Flares	312	166	267	318	
Malfunctioning (CI + U&V)	36	19	30	24	
% Malfunction	11.5%	11.4%	11.2%	7.5%	10.3%
% Unlit and Venting	4.2%	6.0%	4.5%	4.4%	4.6%

The overall malfunction rate of the Repeat Area Survey was similar to the Random Surveys of ~10%; however, the Systematic Survey found a much higher rate of unlit flares at nearly 25%. Reasons for this large increase in unlit flares is unclear. This area was also observed to have a much lower rate of active flares (~50%) than both the Repeat Area Survey (~66%) and the Random Surveys (~89%). Notably, the Systematic Survey occurred in an area of the basin with lower oil and gas production than the Repeat Area Survey. The reduced production and therefore intermittency in which these sites need to flare gas

could lead to a higher rate in their malfunctions, yet more analyses are to be performed to confirm such a hypothesis and estimate the resulting impact on emissions from this comparison.

Interpreting the results of the Repeat Area Survey, about ¼ of the flares with malfunctions (6/23) persisted for all three survey days, while over half of these flares (13/23) showed at least two malfunctions during the survey. Although this is a small sample set of flares observed in the basin, the variability in flare performance was dominantly episodic with difficult to assess mechanisms.

Table 2: Summary of ‘Systematic’ and ‘Repeat Area’ Flaring Survey Observations

	Systematic Survey	Repeat Area Day 1	Repeat Area Day 2	Repeat Area Day 3	Combined Repeat Area Results
Operational	85	115	119	123	357
Inactive	117	69	66	71	71
Combustion Issue	5	6	8	6	20
Unlit and Venting	29	7	8	4	19
Not Surveyed*	0	7	3	0	10
Active Flares	119	128	135	133	396
Malfunctioning (CI + U&V)	34	13	16	10	39
% Malfunction	28.6%	10.2%	11.9%	7.5%	9.8%
% Unlit and Venting	24.4%	5.5%	5.9%	3.0%	4.8%

**On the first day of the Repeat Area Survey, LSI failed to observe two well pads containing seven total flares. One well pad containing four flares was found on the second day; and the other, with three flares, was observed on the final day. No malfunctions were observed on these seven flares when they were surveyed; however, we recognize their absence may play a role in the precise variability of flare malfunctions. We note that regardless of their status on the earlier days, the main conclusion of dominantly episodic malfunctions would still hold true.*

As explained above, Survey 5 expanded the protocol to use OGI to capture emissions from additional types of O&G infrastructure beyond flares. Table 3 below summarizes these observations by emission source, indicating that thief hatches (33%) or other types of vents on storage tanks (46%) represent the dominant emission point within the dataset – as was the case for prior work²⁹.

Table 3: Survey 5 Prevalence of Emission Points

Infrastructure	Number of Emission Points Observed	Percent of Total
Thief Hatch	77	33%
Enardo valve or Vent	109	46%
Flare	37	16%
Other	12	5%
All Sources	235	
Tank Sources	186	79%

For the complex wellpads surveyed during the first 5 days of the survey, production characteristics were aggregated for all wells within 100m of the GPS pin dropped by the helicopter team. Classification of marginal vs non-marginal wells followed the criterion of 15 barrels-of-oil equivalent (BOEd) production using the last 12 months of production if available (or the 2nd month of production if the well had been producing for less than 12 months) using production data¹⁰ complete through January 2021. Table 4 summarizes these results, finding a reduced but still significant prevalence of OGI-detectible emissions at complex marginal wellpads.

Table 4: Emissions by Complex site production characteristics

Site Type	Number of Sites Surveyed	Number of sites with emissions detected	Percent of sites emitting
Complex marginal wellpad	302 (79%)	48	16%
Complex non-marginal wellpad	26 (6.8%)	8	31%
Unable to link to Production	56 (15%)	11	20%
All complex Sites	384	67	17%

Since the helicopter team was counting all flares encountered during the survey and recording their malfunctions, the flaring performance of sites on this survey can be examined similar to prior helicopter surveys. Overall, 15% of active flares were found to be malfunctioning on this survey; however, the performance of flares differs substantially based on the survey guidelines. During the first 5 days of the survey when either systematically looking at all wellpads in a given area or those targeted to be complex marginal sites, the malfunction rate was 36%. This is of similar magnitude to the systematic survey conducted in June 2020, where 29% of flares were malfunctioning; suggesting that intermittent or operational flares are failing at an exceedingly high rate. Alternatively, when using the latest VIIRS data to target routine flaring sites from the prior month, only 5 malfunctions were observed leading to a 3.3% malfunction rate, significantly lower than the range of 7.5% - 11.5% observed in 2020.

Table 5: April 2021 Flaring Survey Results

	All sites	Systematic or complex marginal wellpad survey (Days 1-5)	Routine Flaring Sites (Day 6)
Lit flares	203	56	147
Inactive flares	151	137	14
Percentage of active flares	61.4%	39.1%	91.6%
Malfunctions (Unlit + CI)	37	32	5
Active flare malfunction rate	15%	36%	3.3%

Emissions Estimates from Flaring:

To estimate methane emissions from flaring, the VIIRS Nightfire data²⁷ was aggregated to estimate monthly flared gas volumes from within the spatial extent of the Permian basin and several sub-regions.

The daily observations for source temperatures in the range of 1400 to 2500 K are used and the empirical relationship below is followed²⁵:

$$V_{\text{flared}} = 0.0274RH'$$

Here V_{flared} is the gas flared volume in billions of cubic meters (bcm) and RH' is the average adjusted radiant heat of the observed flares, adjusted to account for the observed non-linearity in the relationship between flared gas volumes and radiant heat parameters. Using this approach, mean flaring volumes in the Permian Basin are estimated at 7.9 bcm (or 280 bcf) in 2019, with 6.5 bcm (230 bcf) in the Texas portion of the Permian and the remainder (1.4 bcm or 49 bcf) in the New Mexico Permian Basin.

For this analysis it is first assumed that operational flares perform at the EPA default combustion efficiency of 98%³¹, which means 2% of the methane sent to the flare is emitted rather than being combusted to carbon dioxide. Unlit flares have a combustion efficiency of 0% since all the methane is emitted unburnt. For the flares that were lit, but with apparent combustion issues, 90% combustion efficiency is assumed. These combined estimates of combustion efficiency combined with our observations of the prevalence of malfunctioning flares lead to an overall combustion efficiency of ~93%, indicating 7% of flared methane is emitted (Table 1). Applying 93% combustion efficiency to the 280 bcf of gas flared in the Permian in 2019 (assuming 80% CH₄ content) results in annual methane emissions of approximately 300,000 metric tons (MT) from flaring in the Permian; unlit flares account for approximately 65% of these emissions, while operational and poorly combusting flares account for about 25% and 10%, respectively. Based on the state-specific flared gas volumes, Texas and New Mexico are responsible for about 250,000 and 50,000 MT of CH₄ emissions, respectively. In comparison, applying the EPA default assumption combustion efficiency of 98% results in about 80,000 – 90,000 MT CH₄ emissions. Our emissions estimate is about 3.5 times higher than alternative estimates based on EPA assumptions of combustion efficiency. EPA publishes two separate estimates of Permian flaring methane emissions, which incorporate the 98% combustion efficiency, but different gas flared data. The 2020 EPA Greenhouse Gas Inventory³² reports 2018 Permian Basin methane emissions of 12,100 MT CH₄ from associated gas flaring, plus 8,500 MT and 4,600 MT from associated gas venting and miscellaneous production flaring, respectively. For comparison, the EPA Greenhouse Gas Reporting Program¹⁷ reports 18,800 MT CH₄ from Permian Basin onshore production facilities.

Regional Emissions Estimates

Atmospheric [CH₄] Transport Modeling:

An atmospheric reanalysis similar to previous studies^{33, 34} was used to create simulated regional atmospheric [CH₄] estimates simulating only atmospheric [CH₄] from emissions within the 100 x 100km Delaware basin study area. Preliminary estimates of surface fluxes of [CH₄] within the Delaware study area were taken from the EPA 2012 gridded inventory³⁵, save for the Permian Basin where an updated, production-based inventory is used³⁶. The Weather Research and Forecasting – Chemistry model (WRF-CHEM)³⁷ was used to simulate atmospheric transport of gases in the reanalysis system; creating a first

estimate of atmospheric [CH₄] consistent with the regional meteorology and the preliminary estimate of emission sources. This reanalysis is incorporated within both aircraft and tower-based quantification of regional CH₄ emissions from the Delaware study area as described in the sections below.

Aircraft-Based Regional Emissions Quantification:

As mentioned briefly above under Aerial Surveys, monthly regional mass balance flights operated by Scientific Aviation were conducted to constrain CH₄ emissions from a high production segment of the Delaware basin, referred to as the Delaware study area. On each flight day, two laps consisting of a box enclosing the 100 km x 100 km Delaware basin study area were flown at 1100 ±100 ft above ground level (agl), with one complete lap taking ~ 2 hours to complete. Two to three vertical profiles were also flown by the aircraft as pairs of ascents/descents to determine the mixing height of surface emissions. Meteorological conditions, [CH₄] measured along the flight path and the mixing height determined from the airborne vertical profiles are synthesized in the mass balance method to calculate CH₄ emissions from the area encircled by the flight path. The large area of the flight path (10,000 km²) combined with atmospheric variability leads to large uncertainties in the emissions quantified utilizing only the direct measurements from the mass balance approach; however, these uncertainties are addressed by incorporating the transport modeling discussed above within the emissions estimate.

CH₄ emissions are computed from each complete circuit by comparing the observed and simulated [CH₄] enhancement, the increase in [CH₄] downwind of the study area relative to a background value and adjusting emissions within the study area to minimize the absolute error between the simulated and observed [CH₄]. The 10th percentile of [CH₄] observations in the circuit determines the background and is subtracted from the observed [CH₄] observations, resulting in an estimate of [CH₄] enhancements. These observed enhancements are then compared to simulated [CH₄] enhancements by matching observation and model at the nearest grid points in space and time. Simulated enhancements are split into two categories: Delaware study area enhancements and enhancements originating from outside the Delaware study area. Enhancements associated with sources outside the Delaware study area are subtracted from the observed [CH₄] enhancements, resulting in a set of observations whose enhancements can be directly attributed to emissions within the Delaware study area. The simulated Delaware study area enhancements are then compared to the observed enhancements, and a scalar multiplier is applied to the simulated enhancements to minimize the absolute error between the two datasets. Because the emissions scale linearly with the simulated enhancements, this scalar multiplier, applied to the preliminary emissions estimate within the study area, provides a solution to the emissions within the Delaware study area. The solution for each of the two circuits are merged into a single daily estimate.

To test the uncertainty of the emission rate solution for each flight day, a 1000-iteration Monte Carlo uncertainty assessment was performed, adjusting various parameters to test how they impacted the solution. This includes the uncertainty in the background, uncertainty in the assumed influence from sources outside the domain and uncertainty in the atmospheric transport. From the 1000 iterations, the 2.5th and 97.5th percentile of solutions are chosen to represent the 95% confidence interval.

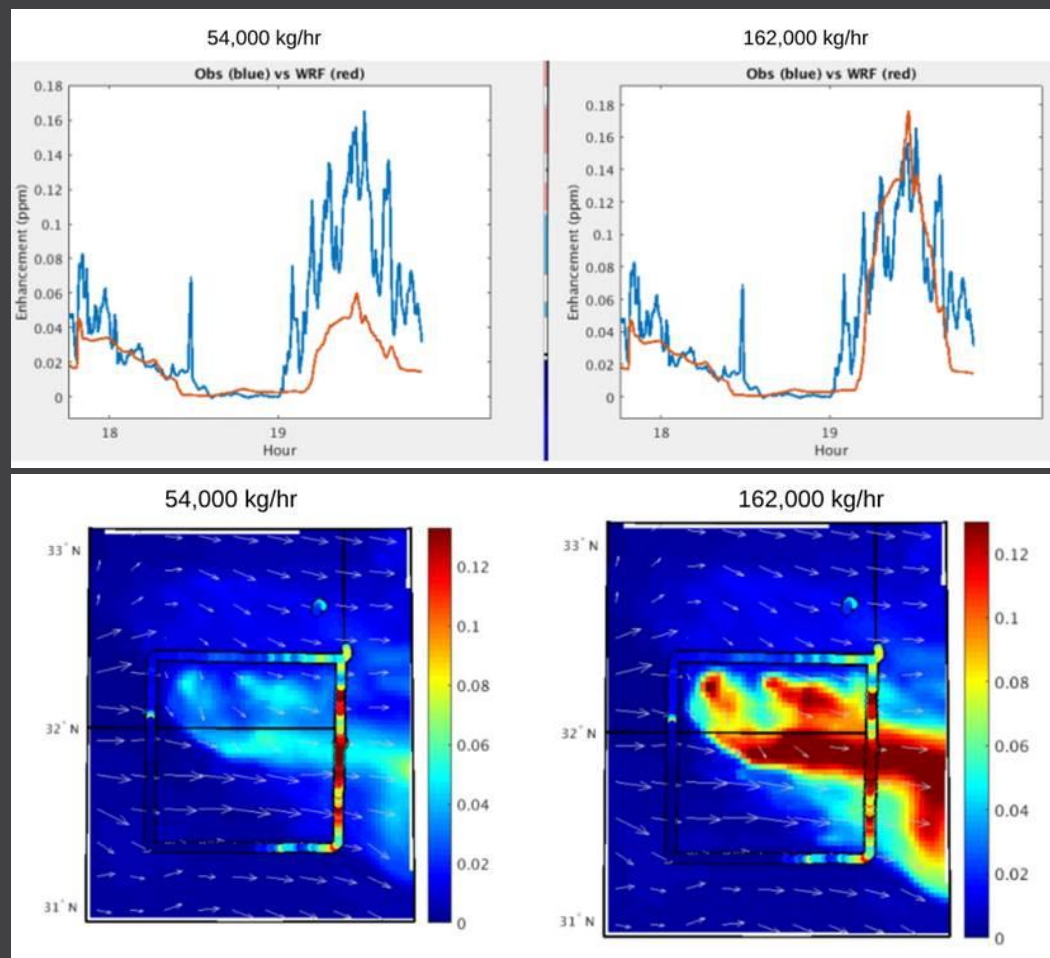
March 9, 2020 Study-Area Loss Rate:

On March 9, Scientific Aviation utilized the mass balance method to quantify emissions from the Delaware study area. $[\text{CH}_4]$ in parts per million over background along the flight paths is shown in Figure 1 below. $[\text{CH}_4]$ is substantially higher in the eastern transect, which is due to methane emissions from within the Delaware study area dispersing downwind. Based on the traditional mass balance approach without utilizing the atmospheric chemistry model, emissions from the Delaware study area were estimated to be $\sim 160,000$ kg CH_4/hr . Atmospheric transport modeling optimizes the fit from the prior inventory²¹ (54,000 kg CH_4/hr) upwards by a factor of three to 162,000 kg CH_4/hr . Figure 1 presents temporal (top) and spatial (bottom) comparisons of the emissions simulated by the prior (left) and posterior (right) conditions. The posterior solution shows marked spatiotemporal agreement with the aircraft observations. The close agreement between the mass balance methodology with and without the transport model supports that methane emissions from the Delaware basin study area on March 9 were approximately 160,000 kg CH_4/hr . Scientific Aviation also completed two other mass balance flights of the study region on January 22, 2020 and March 25, 2020, which had higher uncertainty due to less stable meteorological conditions; however, analyses for these flight show a similar magnitude of emissions to the March 9 flight.

To calculate a loss rate (CH_4 emissions normalized to methane production) in our study area, Enverus data was used to determine all wells in the study area with production during October 2019 – February 2020. As of April 1, 2020, January 2020 was the most recent month with nearly complete production data at the time of this analysis (April 2020). Therefore, January 2020 production was selected as most representative of the March 9 flight. January daily average gas production for all wells within the flight path was spatially aggregated using data provided by Enverus Drillinginfo¹⁰. This gas production value of $\sim 7,300,000$ mcf/day is into a methane production value of 4,672,000 kg CH_4/hr based on assumptions of 80% methane content and 19.2 kg CH_4/mcf . Emissions of 162,000 kg CH_4/hr is equivalent to about 3.5% of total CH_4 production.

Our loss rate estimate for the Permian Basin is substantially higher than the national average. The draft EPA 2020 Greenhouse Gas Inventory (GHGI)³² estimates national O&G supply chain methane emissions are 7.1 Tg, equivalent to approximately a 1.3% loss rate. Our study area contains limited transmission and local distribution, so it is more appropriate to compare to only the production, gathering, and processing segments — which is $\sim 1.1\%$ in the draft 2020 GHGI. Consequently, our measurement-based estimate is about 3 times higher than the average reported by the EPA inventory. In comparison, a synthesis study³⁸ that used site and basin-level data found national average oil and gas supply chain methane emissions to be 13 Tg/yr, or a 2.3% loss rate; for production, gathering and processing, the loss rate is $\sim 2.0\%$. Accordingly, the Permian loss rate is about 75% higher than this current best estimate of national emissions.

Figure 1. Prior (left) and posterior (right) modeled and measured methane enhancement (concentration in parts per million over background) for the March 9th flight. The colors in the square perimeter represent measured methane enhancement from Scientific Aviation’s flight around the study area. The bottom figures show that the prior inventory of 54,000 kg/hr is inaccurate because modeled and observed enhancement do not match, yet tripling the inventory (162,000 kg/hr) results in a match.



Tower Based Regional Emissions Quantification:

Continuous measurements of atmospheric [CH₄] and [CO₂] were collected at five locations surrounding the Permian Basin Study Area beginning March 1, 2020 using methods similar to a prior study³⁴. Note that only four of the five planned measurement sites are used in this analysis for months prior to September 2020 due to intermittent instrument malfunctions at the northernmost site (Maljamar). Of these measurement locations, four were on towers at measurement heights of 80 – 134 m agl and the westernmost site (Carlsbad) was at a mountaintop station on a rooftop of 4 m agl. The measurements were made with wavelength-scanned cavity ring down spectroscopic instruments (Picarro, Inc., models G2301, G2401, G2204, and G2132-i). The air samples were dried using Nafion dryers (PermaPure, Inc.) in reflux mode, with an internal water vapor correction applied for the effects of the remaining water vapor (< 1 %). The instruments were calibrated in the laboratory prior to deployment and using quasi-

daily field tanks traceable to the WMO X2004A scale^{39, 40}. The [CH₄] measurement uncertainty (including instrument noise, uncertainty due to water vapor calibration and tank assignment uncertainty) for the tower locations ranged from 0.6-5.4 ppb, with the differences being attributable to different instrument type, short Nafion dryer (Hobbs), and laser aging (Notrees).

[CH₄] emissions in the study domain were calculated for each day of tower observations using a similar technique as used with the aircraft observations described above. Daily afternoon [CH₄] at each tower site averaged from 16Z (11 LST) through 22Z (17 LST) was computed from both the observations and the simulation. A background [CH₄] value (for both the observations and the model) was selected based on the lowest measurement from the available tower sites. This background was subtracted from all tower sites to create an observed [CH₄] enhancement, from which simulated enhancements from sources outside of the Delaware study area were subtracted to produce an observed [CH₄] enhancement associated with sources inside the Delaware study area. A scalar multiplier was then applied to minimize the absolute error between the observed and modelled enhancements, and a daily emission rate was solved for in the Delaware study area.

Unlike the aircraft observations, which are collected on days where meteorological conditions are ideal for measuring emissions from the study domain, the tower dataset is continuous, and many days may not be suitable for calculating an emission rate from the Delaware study area. The most useful tower observations for solving for emissions within the Delaware study area are those whose enhancements are influenced primarily by sources within the Delaware study area and contain minimal enhancements from sources outside of the Delaware study area. These conditions are selected for by retaining days when >50% of the simulated downwind afternoon tower enhancements come from sources within the Delaware study area.

The resulting timeseries of emissions is presented at two temporal scales. First, a 'weekly moving average' is calculated numerically as a 7-datapoint moving average of the emissions days that are retained after filtering those with unsatisfactory conditions to constrain emissions within the study area. Additionally a 'monthly mean' emission estimate is calculated for all retained days for a given month. New results are added to the available dataset monthly, approximately 3 weeks after the end of each month. Complete results from the tower analyses and aircraft-based regional quantification are available on the platform for view; additional methodological details and resulting implications from these data through the Summer of 2020 can be found in a peer reviewed publication⁴¹.

Uncertainty, Detection Limits, and Scale:

As with any emission estimation technique, the approaches used by Scientific Aviation and University of Wyoming have both uncertainty and minimum detection limits. Uncertainty refers to the accuracy (how close to the actual value) and precision (consistency) of measurements. The Minimum Detection Limit (MDL) is the smallest emission rate that an approach can quantify with enough precision to determine if it is statistically significant from zero. The uncertainty and MDL of the mass balance, OTM 33A and transect approach have been tested with two basic techniques: 1) controlled release tests, and 2) uncertainty propagation. Single blind controlled releases can be used to empirically test the accuracy,

precision and probability of detection at different emission rates and conditions. Uncertainty propagation uses statistical techniques to estimate total uncertainty of an estimate from the uncertainty of input parameters such as wind speed. Based on controlled releases, Scientific Aviation’s mass balance approach for small areas can detect emissions as small as 5–10 kg CH₄/hr with 10% uncertainty during optimal conditions. However, based on uncertainty propagation, the Permian project measurements have a median uncertainty closer to ±60% with few measurements less than 40 kg CH₄/hr being statistically significant from zero. This higher uncertainty and detection limit are likely due to the high density of methane sources, which increases the variability of upwind methane concentrations. OTM 33A can detect much smaller emissions down to 0.036 kg CH₄/hr with +233%/-41% uncertainty. Although the OTM 33A has relatively poor precision, controlled tests have shown it has little bias, which means it can be used to accurately characterize a population with a large enough sample size.

On the PermianMAP operator dashboard⁹, measured areas are presented using a colored scale with five bins based on absolute emission rates in kg CH₄/hr: 1) White: <2 kg CH₄/hr; 2) Yellow: 2 – 100 kg CH₄/hr; 3) Orange: 100 – 1000 kg CH₄/hr; 4) Red: >1000 kg/hr; and 5) Grey: Uncertain. For context, previous studies^{32, 42} estimate that the average U.S. well emits between 1 – 2 kg CH₄/hr. The gray “uncertain” bin includes aerial survey measurements where it could not be determined that the emissions were above zero within a 1σ uncertainty bound. Due to the complexity of the Permian environment, preliminary data indicate the detection limit for Scientific Aviation’s aerial measurements may be as high as ~40 kg CH₄/hr under certain conditions. Therefore, it is possible that measurement areas labeled “uncertain” could have relatively high emissions that were unable to be quantified due to issues such as interfering sources and poor meteorological conditions at time of measurement.

Data Availability:

All data collected through the surveys, including estimated emission rates and associated uncertainty, are available from the ‘Download Datasets’ tab available on the main platform site⁹. For questions about the data presented on the platform and in this document please contact permianmap@edf.org.

References:

- ¹ Cusworth, D. H., et al., Intermittent Methane Emissions in the Permian Basin, *Environmental Science & Technology Letters*, 2021, <https://doi.org/10.1021/acs.estlett.1c00173>
- ² Duren, R. M., et al., California's methane super-emitters, *Nature*, 7781, 180-184, 2019, <https://doi.org/10.1038/s41586-019-1720-3>
- ³ Frankenberg, C., et al., Airborne methane remote measurements reveal heavy-tail flux distribution in Four Corners region, *Proceedings of the National Academy of Sciences*, 35, 9734-9739, 2016, <https://doi.org/10.1073/pnas.1605617113>
- ⁴ Thorpe, A. K., et al., Mapping methane concentrations from a controlled release experiment using the next generation airborne visible/infrared imaging spectrometer (AVIRIS-NG), *Remote Sensing of Environment*, 104-115, 2016, <https://doi.org/10.1016/j.rse.2016.03.032>
- ⁵ Methane Source Finder, <https://methane.jpl.nasa.gov/>
- ⁶ CarbonMapper, <https://carbonmapper.org/>
- ⁷ ASOS Network, 2021, <https://mesonet.agron.iastate.edu/ASOS/>
- ⁸ High-Resolution Rapid Refresh, <https://rapidrefresh.noaa.gov/hrrr/>
- ⁹ Environmental Defense Fund, PermianMAP, <https://data.permianmap.org/pages/operators>
- ¹⁰ Enverus, Drillinginfo, <https://www.enverus.com>
- ¹¹ Railroad Commission of Texas (RRC), Production Data, Oil & Gas Well Data, <https://www.rrc.state.tx.us/about-us/resource-center/research/data-sets-available-for-download/>
- ¹² New Mexico Oil Conservation Division (NMOCD), OCD Geographic Information Systems, <https://www.emord.state.nm.us/OCD/ocdgis.html>
- ¹³ New Mexico Environment Department (NMED), Air Facilities, <https://data-nmenv.opendata.arcgis.com/datasets/4d92b3af492e49688b14e711fbf83129?showData=true>
- ¹⁴ Texas Commission on Environmental Quality (TCEQ), Air Permitting, https://www.tceq.texas.gov/permitting/air/air_permits.html
- ¹⁵ Scientific Aviation, <https://www.scientificaviation.com/methods/>
- ¹⁶ Descartes Labs, <https://www.descarteslabs.com/industries/oil-and-gas/>
- ¹⁷ United States Environmental Protection Agency (USEPA), Greenhouse Gas Reporting Program, <https://ghgdata.epa.gov/ghgp/main.do>
- ¹⁸ Thoma, E. S., B., OTM 33 Geospatial Measurement of Air Pollution, Remote Emissions Quantification (GMAP-REQ) and OTM33A Geospatial Measurement of Air Pollution-Remote Emissions Quantification-Direct Assessment (GMAP-REQ-DA), <https://www3.epa.gov/ttnemc01/prelim/otm33.pdf>
- ¹⁹ Brantley, H. L., et al., Assessment of Methane Emissions from Oil and Gas Production Pads using Mobile Measurements, *Environmental Science & Technology*, 24, 14508-14515, 2014, <https://doi.org/10.1021/es503070g>
- ²⁰ Robertson, A. M., et al., Variation in Methane Emission Rates from Well Pads in Four Oil and Gas Basins with Contrasting Production Volumes and Compositions, *Environmental Science & Technology*, 15, 8832-8840, 2017, <https://doi.org/10.1021/acs.est.7b00571>
- ²¹ Caulton, D. R., et al., Quantifying uncertainties from mobile-laboratory-derived emissions of well pads using inverse Gaussian methods, *Atmos. Chem. Phys.*, 20, 15145-15168, 2018, <https://doi.org/10.5194/acp-18-15145-2018>
- ²² Edie, R., et al., Constraining the accuracy of flux estimates using OTM 33A, *Atmos. Meas. Tech.*, 1, 341-353, 2020, <https://doi.org/10.5194/amt-13-341-2020>
- ²³ Edie, R., et al., Off-Site Flux Estimates of Volatile Organic Compounds from Oil and Gas Production Facilities Using Fast-Response Instrumentation, *Environmental Science & Technology*, 3, 1385-1394, 2020, <https://doi.org/10.1021/acs.est.9b05621>
- ²⁴ SkyTruth, Global Flaring Dataset, <https://skytruth.org/flaring/>

- ²⁵ Elvidge, C. D., et al., Methods for Global Survey of Natural Gas Flaring from Visible Infrared Imaging Radiometer Suite Data, *Energies*, 1, 14, 2016, <https://doi.org/10.3390/en9010014>
- ²⁶ Elvidge, C. D., Zhizhin, M., Hsu, F.-C. and Baugh, K. E., VIIRS Nightfire: Satellite Pyrometry at Night, *Remote Sensing*, 9, 4423-4449, 2013, <https://doi.org/10.3390/rs5094423>
- ²⁷ Earth Observation Group, Payne Institute for Public Policy, Colorado School of Mines., VIIRS Nightfire, <https://payneinstitute.mines.edu/eog-2/viirs/>
- ²⁸ Leak Surveys Incorporated (LSI), <https://www.leaksurveysinc.com/>
- ²⁹ Lyon, D. R., et al., Aerial Surveys of Elevated Hydrocarbon Emissions from Oil and Gas Production Sites, *Environmental Science & Technology*, 9, 4877-4886, 2016, <https://doi.org/10.1021/acs.est.6b00705>
- ³⁰ Sierra-Olympic Technologies, <https://sierraolympic.com/thermal-cameras-mwir/ventus-ogi/>
- ³¹ eCFR Title 40 Section 98.233(n)(5), <https://ecfr.io/Title-40/Section-98.233>
- ³² United States Environmental Protection Agency, Inventory of U.S. Greenhouse Gas Emissions and Sinks: Natural Gas and Petroleum Systems, <https://www.epa.gov/ghgemissions/natural-gas-and-petroleum-systems>
- ³³ Barkley, Z. R., et al., Estimating Methane Emissions From Underground Coal and Natural Gas Production in Southwestern Pennsylvania, *Geophysical Research Letters*, 8, 4531-4540, 2019, <https://doi.org/10.1029/2019GL082131>
- ³⁴ Barkley, Z. R., et al., Quantifying methane emissions from natural gas production in north-eastern Pennsylvania, *Atmospheric Chemistry and Physics*, 22, 13941-13966, 2017, <https://doi.org/10.5194/acp-17-13941-2017>
- ³⁵ Maasackers, J. D., et al., Gridded National Inventory of U.S. Methane Emissions, *Environmental Science & Technology*, 23, 13123-13133, 2016, <https://doi.org/10.1021/acs.est.6b02878>
- ³⁶ Zhang, Y., et al., Quantifying methane emissions from the largest oil-producing basin in the United States from space, *Science Advances*, 17, eaaz5120, 2020, <https://doi.org/10.1126/sciadv.aaz5120>
- ³⁷ Skamarock, W. C., et al., G.: A description of the Advanced Research WRF version 3, Citeseer, 2008, <https://doi.org/10.5065/D68854MVH>
- ³⁸ Alvarez, R. A., et al., Assessment of methane emissions from the U.S. oil and gas supply chain, *Science*, 6398, 186, 2018, <http://science.sciencemag.org/content/361/6398/186.abstract>
- ³⁹ Richardson, S. J., et al., Tower measurement network of in-situ CO₂, CH₄, and CO in support of the Indianapolis FLUX (INFLUX) Experiment, *Elementa: Science of the Anthropocene*, 2017, <https://doi.org/10.1525/elementa.140>
- ⁴⁰ National Oceanic and Atmospheric Administration (NOAA), Methane (CH₄) WMO Scale, https://www.esrl.noaa.gov/gmd/cc1/ch4_scale.html
- ⁴¹ Lyon, D. R., et al., Concurrent variation in oil and gas methane emissions and oil price during the COVID-19 pandemic, *Atmos. Chem. Phys.*, 9, 6605-6626, 2021, <https://doi.org/10.5194/acp-21-6605-2021>
- ⁴² Omara, M., et al., Methane Emissions from Natural Gas Production Sites in the United States: Data Synthesis and National Estimate, *Environmental Science & Technology*, 21, 12915-12925, 2018, <https://doi.org/10.1021/acs.est.8b03535>